ELSEVIER

Journal of Power Sources 112 (2002) 236–246

JOURNAL OF POWER SOURCES

www.elsevier.com/locate/jpowsour

Comparison of commercial supercapacitors and high-power lithium-ion batteries for power-assist applications in hybrid electric vehicles I. Initial characterization

Andrew Chu*, Paul Braatz

HRL Laboratories, LLC 3011, Malibu Canyon Road, Malibu, CA 90265-4797, USA

Received 24 June 2002; accepted 30 June 2002

Abstract

Commercial supercapacitors, also known as ultracapacitors or electrochemical capacitors, from Saft, Maxwell, Panasonic, CCR, Ness, EPCOS, and Power Systems were tested under constant current and constant power discharges to assess their applicability for power-assist applications in hybrid electric vehicles (HEVs). Commercial lithium-ion batteries from Saft and Shin-Kobe were also tested under similar conditions. Internal resistances were measured by electrochemical impedance spectroscopy (EIS), as well as by the ''*iR* drop'' method. Self discharge measurements were also recorded. Compared with earlier generations of supercapacitors, the cells showed improved current and power capability. However, their energy densities are still too low to meet goals set by Partnership for a New Generation of Vehicles (PNGV) for HEV propulsion. Cells that use acetonitrile as the electrolyte solvent yield better performance, although safety issues need to be addressed. New high-power lithium-ion batteries show high energy densities, with high power capabilities.

Keywords: Hybrid electric vehicles; Electrochemical impedance spectroscopy; High-power lithium-ion batteries

1. Objective

The purpose of this study is to assess the capability of commercial supercapacitors for use in hybrid electric vehicles (HEVs). The experimental methodologies used, however, are quite general and the results of this study may be applied to other high-power applications with time scales of 1 to >100 s.

2. Introduction

The problem of limited driving range in electric vehicles (EVs) has prompted development of hybrid electric vehicles that use a fuel-efficient, lean-burning engine, in combination with a battery and electric drivetrain.[1] The batteries provide power for acceleration and capture energy during regenerative braking. Unfortunately, fast discharging and charging lead to reduced cycle life and performance in traditional batteries. As a result, batteries must be oversized to supply the high current, power bursts required for vehicle propulsion, adding unnecessary weight to the system.

One alternative to batteries is to have supercapacitors supply the bursts of power. A supercapacitor is an energy storage device with behavior somewhere between a battery and a traditional capacitor. It is also called an ''ultracapacitor'' or more generally, an ''electrochemical (EC) capacitor.'' It can be charged and discharged quickly like a capacitor, but exhibits 20–200 times greater capacitance than conventional capacitors [1]. The supercapacitor can supply the power needed during vehicle acceleration and capture energy during regenerative braking. At cruising speeds, a fuel-efficient engine charges the supercapacitor and provides the power needed for propulsion.

In comparison with batteries, supercapacitors achieve higher power density but lower energy density. The difference stems from a different mechanism of energy storage [1]. Batteries store energy by redox reactions in the bulk electrode, leading to high energy density but slow kinetics. The higher rate capability of supercapacitors comes from the electrostatic storage of charge at the electrode surface. The transport of ions in the solution to the electrode surface is rapid, leading to fast charge and discharge capability. In

* Corresponding author. Tel.: +1-310-317-5325; fax: +1-310-317-5484.
E-mail address: achu@hrl.com (A. Chu).

[1] Supercapacitors could also be used in hybrid systems with fuel cells, which are limited in their ability to deliver large current pulses.

0378-7753/02/$ – see front matter
PII: S0378-7753(02)00364-6

contrast to batteries, no electron transfer takes place across the interface. Supercapacitors can be fully charged or discharged within a few seconds without damaging the cell and thus are well suited for use in power-assist applications in vehicle propulsion. The charging and discharging processes are highly reversible and do not require phase changes in the electrodes. This should lead to increased cycle life, compared to batteries.

Most of the attention in supercapacitors for hybrid electric vehicles has been focused on carbon-based cells with non-aqueous electrolyte. Currently, these cells offer the best performance at the lowest cost and have been produced in large cells suitable for automotive applications. In 1998, Wright and Murphy [2,3] published studies on carbon-based capacitors from Maxwell and Saft. These thorough studies include a large amount of testing data for cells produced a few years ago. At that time, the specific energy and specific power of all cells studied were well below the goals set by Partnership for a New Generation of Vehicles (PNGVs).[2] With each year, however, the technology has progressed: energy and power densities have increased, while RC time constant has decreased.

Recent reports indicate that significant improvements have been made in commercial supercapacitor devices [4–6]. Burke et al. report that technologies have been developed that can achieve both high energy density (>5 W h/kg) and high power density (>2 kW/kg) [4]. In addition to improvements in commercial cells from well-established producers, such as Maxwell, Panasonic, and Saft, relative newcomers, such as Ness Corporation (Korea) have shown very exciting results in large cells suitable for use in vehicles [4].

In comparing test data on supercapacitors from different manufacturers, it should be recognized that they were not all optimized for hybrid electric vehicle propulsion. Consequently, performance data reported here are not necessarily indicative of their relative merits for other applications. When comparing energy and power density data from supercapacitors or other energy storage devices, it is important to have a consistent basis for comparison [5]. For automotive applications, a cell must have high power density and a high efficiency. Maximum power density, calculated from matched impedance pulses with a discharge efficiency of 50%, is a useful measure but does not reflect the requirements of hybrid vehicle applications which typically demand at least 90% efficiency. Many pulse batteries, for example, may show high energy density and high pulse power density, but not simultaneously. Internal resistance in the cell leads to ohmic losses and heating when high power pulses are used, leading to decreased efficiency. Supercapacitors, in general, offer lower resistance, and therefore, greater power and efficiency compared to pulse batteries [7].

Conway has written a thorough review of the chemistry of electrochemical capacitors [1]. In addition, Burke has written a report summarizing the status of the technology [5]. The goal of this paper is to provide the latest data and to provide a side-by-side comparison of cells from different manufacturers. It is hoped that this will aid in the development of supercapacitor technology, particularly for automotive applications.

3. Materials and methods

Since the purpose of this study was to assess the use of supercapacitors and lithium-ion batteries for hybrid electric vehicle applications, cost and performance were two important criteria for cell selection. For the supercapacitors, only cells with a capacitance of greater than 1000 F were tested, although it is likely that cells would be 2000 F or larger in actual use. All of the supercapacitor cells tested have carbon-based electrodes and an organic electrolyte. In addition, all are commercially available or can be produced in large quantities. Thus, there is the potential that the cost per unit would be reasonable if the sales volume were high. Ruthenium oxide-based cells, as well as other cells with more expensive electrode materials, were not considered. Cells were obtained from Maxwell Technologies (San Diego, US), Saft (France), Panasonic (Japan), CCR (Japan), Ness Corporation (Korea), and EPCOS (Germany). The cells were obtained in 2000 or early 2001 and do not reflect the latest improvements which may have been incorporated in more recently-manufactured cells. With respect to the lithium-ion cells, samples from Saft and Shin Kobe were tested because of their availability. A Sony lithium-ion battery designed for commercial electronic devices was also tested for comparison.

One of the tests used to characterize the cell is a series of constant current discharges, at progressively higher rates, which will be referred to as a ‘‘Peukert test’’. The Peukert test measures a cell’s rate capability and is described here. Before each discharge pulse, the cell is charged to the manufacturer-recommended maximum voltage (V_{max}) using a 40 amp charge, followed by a 0.4 amp trickle charge. The applied discharge currents for the cell are: 4, 8, 20, 40, 80, 120, 160 and 200 A, regardless of the size or capacity of the cell. Supercapacitors can be discharged down to 0 V, but are typically discharged to a minimum voltage (V_{min}) set equal to $0.5V_{max}$. Peukert data on lithium-ion batteries will not be presented in this paper.

Another test to characterize the cell is a series of constant power discharges, at progressively higher rates, sometimes called a ‘‘Ragone test’’. This is similar to the Peukert test, but constant power discharges are used rather than constant

[2] Supercapacitors could also be used in hybrid systems with fuel cells, which are limited in their ability to deliver large current pulses. PNGV is a partnership between the United States Government and the US Council for Automotive Research (USCAR) which represents DaimlerChrysler, Ford and General Motors. The goal of PNGV is to develop technology that can be used to create environmentally friendly vehicles that can achieve up to triple the fuel efficiency of today’s vehicles with very low emissions without sacrificing affordability, performance or safety.

current discharges. The applied constant power discharges are the same for all supercapacitor cells: 4, 8, 20, 40, 80, 120, 160 and 200 W. The lithium-ion batteries were tested at the following applied constant power discharges: 5, 10, 20, 30, 50, 100, 150 and 200 W. In the case of lithium-ion, the entire manufacturer-recommended voltage range was used. This difference in voltage range between supercapacitors and lithium-ion batteries is consistent with the guidelines established by PNGV, since this is how they would be used for HEVs. In an actual energy storage system used for vehicle traction, the power electronics are more complicated as the voltage range increases. Therefore, PNGV establishes a maximum voltage range for the energy system.

Constant current and constant power testing was performed on a BT2000 Test Station (Arbin Instruments, College Station, Texas) running MitsPro software. The electrochemical impedance measurements were taken using a Solartron 1287 Electrochemical Test Stand and Solartron 1260 Frequency Response Analyzer (Solartron Instruments, Houston, Texas) running ZPlot 2.0 (Scribner and Associates, Southern Pines, NC).

4. Results

Cells, by manufacturer, cell ID number, mass, nameplate and measured capacitance, manufacturer-recommended maximum voltage, measured capacity and energy are listed in Table 1.

In this study, the measured capacitance, capacity and energy of all supercapacitors are obtained using a slow discharge from V_{max} to $0.5V_{max}$. It should be noted that in the literature, capacitance, capacity and energy data are usually reported between V_{max} and 0 V. A discharge to $0.5V_{max}$ gives 75% of the energy as a discharge to 0 V. Therefore, care should be taken when comparing the numbers between this study and manufacturers' data sheets or other reports in the literature. As a reminder, in the case of the lithium-ion batteries, the entire manufacturer-recommended voltage range was used. The supercapacitor nameplate capacitance is given by the manufacturer. The manufacturer-recommended maximum voltage is an important parameter to note because the capacity and energy measurements necessarily depend on the voltage to which the cell is charged. Most of these cells can be charged to a higher voltage for a short period of time without damaging the cell. However, extended periods of time at elevated voltage are expected to decrease long-term performance.

The Panasonic cells are divided into three groups: UPA, UPB, and UPC. According to the Panasonic product literature, the UPA cell is designed for low current and higher capacity "energy storage" applications. The UPB cell is capable of high current, but with a lower capacity, for "power supply" applications. The UPC cells contain an acetonitrile-based electrolyte.

5. Constant current (Peukert) results

Except for the immediate (iR) drop upon application of the current pulse, the voltage versus time curves for a supercapacitor during a constant current discharge are linear. This is in contrast to the lithium-ion batteries, which has a relatively flat voltage profile curve with sharp changes in voltage when the cell is in the fully charged or discharged condition. The shape of the voltage profile curve is due to the mechanism of energy storage, which differs in these two systems. In supercapacitors, the energy storage is primarily a surface phenomenon where charged species in the electrolyte approach the electrode surface. No charge transfer across the interface occurs; it is a non-Faradic reaction. This allows very fast kinetics, since the movement of ions in the electrolyte is fast. In batteries, the energy storage is due to a redox reaction in the bulk electrodes. This does involve the transfer of charged species across the interface, a Faradic reaction. Since the bulk electrode is used to store charge, the

Table 1
Summary of commercial supercapacitor and Li-ion battery information

Manufacturer	Cell ID	Number of cells	Cell mass (kg)	Nameplate capacitance (F)	Measured capacitance (F)	Measured capacity (A h)	Measured energy (W h)
Saft	SAFT1-6	6	0.648	3500	3,744	1.456	3.017
Maxwell	PC2500A-C	3	0.711	2500	3,269	1.174	2.281
Maxwell	PC2500D-G	4	0.715	2500	3,283	1.140	2.144
CCR	CCR2000A-C	3	0.402	2000	2,124	0.678	1.162
CCR	CCR3000A-C	3	0.500	3000	3,010	0.961	1.648
Panasonic	UPA1-2	2	0.335	2000	1,755	0.561	0.952
Panasonic	UPB1-2	2	0.339	1200	1,019	0.325	0.559
Panasonic	UPC1-2	2	0.308	2000	1,781	0.569	0.956
Ness	NESS1-4	4	0.623	2500	2,501	0.799	1.356
EPCOS	EP12A-B	2	0.441	1200	1,189	0.413	0.779
EPCOS	EP27,1-4	4	0.657	2700	3,034	0.969	1.742
Power System	PSL,1-2	2	0.230	1250	1,312	0.492	1.024
Shin-Kobe	SK1-8	8	0.301	N/A	9,285	3.611	12.483
Saft	HP6A-F	8	0.384	N/A	19,683	7.655	22.263

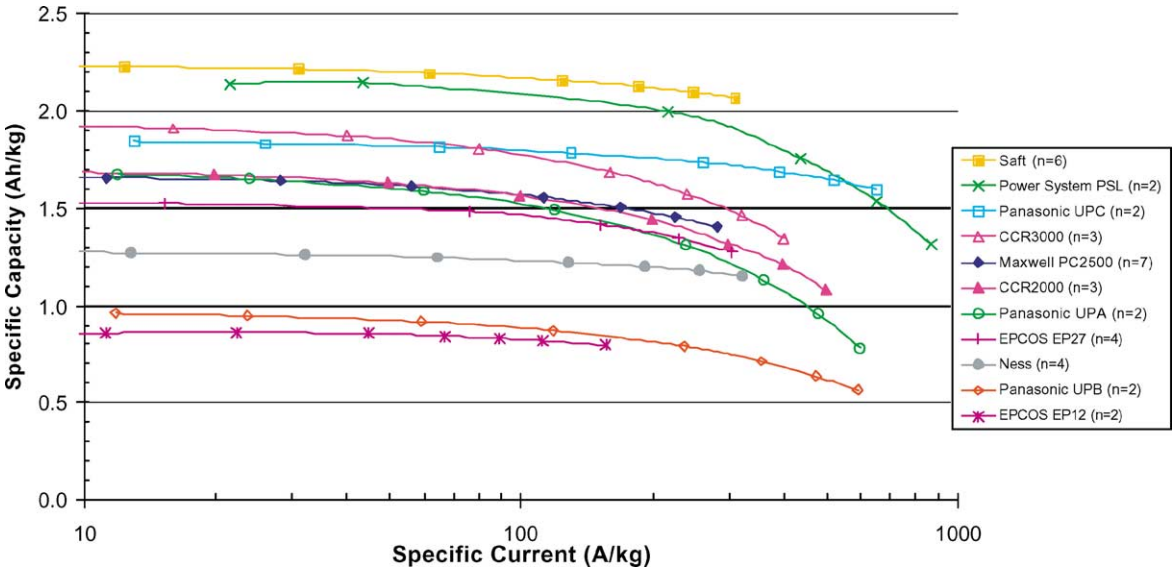

Fig. 1. Peukert plot of HRL data on commercial supercapacitor cells, normalized to total cell weight. The number of cells (n) comprising the average is given in the legend.

energy density is higher but the kinetics are inherently slower, due to diffusion of species in the electrode material.

The capacity at each constant current discharge is recorded, and the capacity is plotted versus the applied current, with the data normalized to the cell mass (see Fig. 1.) In this plot, the curves represent the average of at least two cells. The number of cells (n) comprising the average is given in the legend. This ''Peukert'' plot gives an indication of the rate capability of the cell and allows comparison between cells. The Saft cells showed the highest specific capacity. Panasonic UPC, Maxwell, and CCR and were next. The Ness cells, while having a relatively low specific capacity, showed very good rate capability as seen

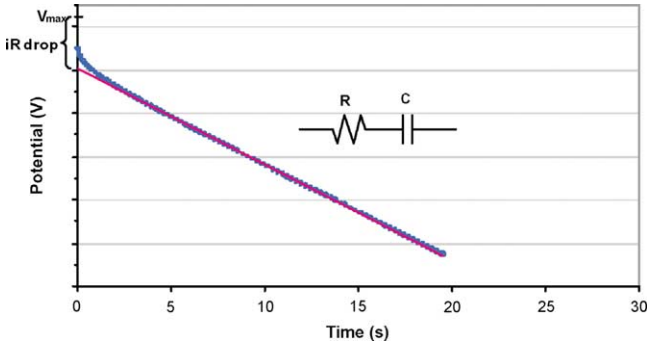

Fig. 2. Comparison of representative constant current discharge data and simple equivalent circuit model.

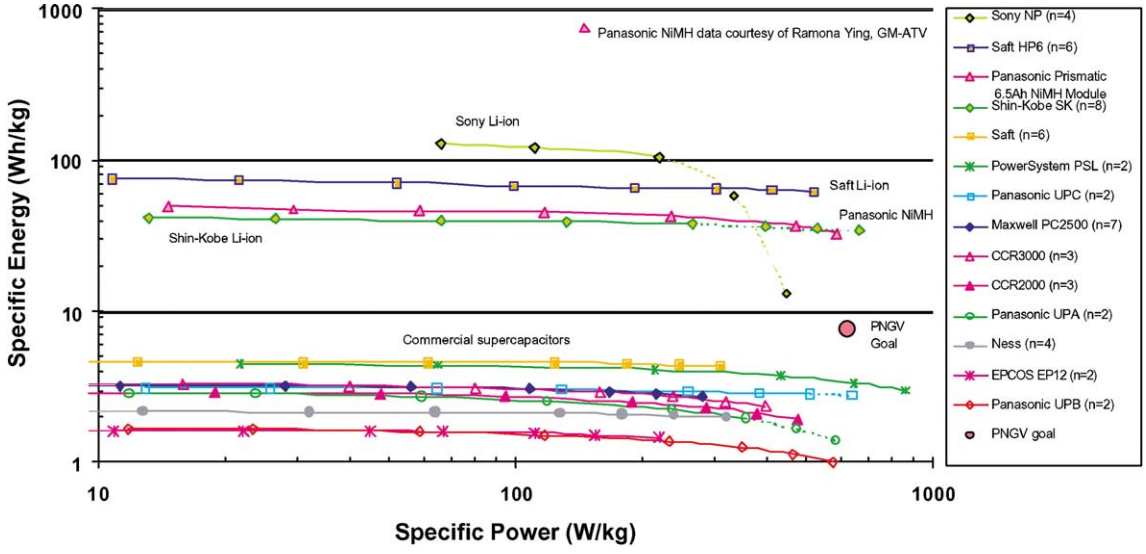

Fig. 3. Ragone plot of HRL-measured data on commercial supercapacitors, normalized to total cell weight. Saft shows the highest specific energy, with Maxwell next. CCR, EPCOS and Panasonic show somewhat lower energy. The PNGV goals for energy and power are included for reference. It should be noted that the constant power discharges were sometimes performed at a level above the manufacturer-recommended current limit. When this was the case, the data are represented by dashed lines.

Table 2
Summary of Peukert data at the lowest and highest current discharge, where n is the number of cells used to obtain the average

Manufacturer	Cell ID (number of cells)	Average specific capacity (A h/kg)	Measured at specific current (W/kg)	Average specific capacity (A h/kg)	Measured at specific current (W/kg)
Saft	SAFT ($n = 6$)	2.24	6.17	2.07	308.5
Maxwell	PC2500 ($n = 7$)	1.65	5.62	1.41	281.2
CCR	CCR2000 ($n = 3$)	1.69	9.95	1.08	497.3
CCR	CCR3000 ($n = 3$)	1.92	8.00	1.34	399.9
Panasonic	UPAN ($n = 2$)	1.84	12.97	1.60	648.5
Panasonic	UPA ($n = 2$)	1.67	11.94	0.78	597.0
Panasonic	UPB ($n = 2$)	0.96	11.81	0.57	590.7
Ness	NESS ($n = 4$)	1.28	6.42	1.15	320.8
EPCOS	EP12 ($n = 2$)	0.78	2.21	0.80	156.5
EPCOS	EP27 ($n = 4$)	1.38	1.53	1.27	304.6
Power System	PSL ($n = 2$)	2.14	21.52	1.31	869.5

by the flat curve (solid circle) in Fig. 1. Panasonic UPB and EPCOS showed the lowest specific capacity with respect to discharge current.

The results of the Peukert tests are summarized in tabular form below (see Table 2). For each cell, the manufacturer's nameplate capacitance is compared to the measured capacitance at the lowest current (4 A) during the Peukert test. From the constant current Peukert data, it is possible to calculate the capacitance of the supercapacitor cell. The following discussion does not apply to lithium-ion batteries. Capacitance is defined as the charge on the capacitor divided by the potential difference:

$$C = \frac{Q}{\Delta V} \tag{1}$$

where C is the capacitance (F), Q the charge on the capacitor (C or A s) and ΔV the potential difference (V).

The capacitance calculated at the slowest constant current discharge (4 A) is included in Table 2. Next, the specific capacities are listed for the lowest (4 A) and highest (200 A) currents during the Peukert test. The corresponding specific currents for those specific capacities are also listed. This is equivalent to taking two data points for each cell from the summary Peukert plot (Fig. 1).

There are two ways of calculating the capacitance from the constant current experiment. The first, previously mentioned, is to measure the total amount of charge (A s) passed during the constant current charge and divide by the change in cell voltage (see Eq. (1)).

The second method of calculating capacitance is by measuring the slope of the linear portion of the voltage profile $V(t)$ curve, which is equal to I/C. Since the applied current is constant, the capacitance simply equals the applied current divided by the slope of the $V(t)$ curve:

$$C = \frac{I_{\text{applied}}}{\text{slope of } V(t) \text{ curve}} \tag{2}$$

This method, of course, relies on voltage profile curves that have a well-defined linear region. Such curve fitting is somewhat arbitrary, since the linear region of the voltage profile curve must be determined before the calculation can be performed. If the curve can be described by an instantaneous drop, followed by a linear discharge, the data can be fitted by an equivalent circuit consisting of a resistor in series with a capacitor (see Fig. 2). The slope of the line is used to calculate the capacitance, using Eq. (2). The iR drop is used to calculate the cell's resistance, using the discharge current ($R = V/I$). The calculated capacitance was found to vary slightly (less than 5%) at the different constant current discharges. This method is somewhat subjective because the data cannot be accurately described by an instantaneous drop followed by a perfectly linear discharge (see Fig. 2). In reality, the discharge curve is smooth with a gradual transition. Nevertheless, to a first-order approximation, this method does yield useful information regarding the capacitance and internal resistance of the cell.

Both methods of calculating the capacitance assume ideal behavior and that the capacitance is not a function of the cell voltage, i.e. it is constant during the experiment. Also, it is possible that the values for resistance and capacitance may differ between charge and discharge. Analysis of the resistance, calculated from the iR drop, generally showed that the largest cells show the lowest internal resistance. This is expected, since the resistance values are not normalized to the cell's surface area. Nonetheless, the Maxwell cells with a similar measured capacitance, and presumably comparable surface area, showed higher internal resistance compared to the Saft cells. The CCR and Panasonic cells showed internal resistance in the 2–3 mΩ range. The EPCOS cells showed a surprisingly low resistance, but the Ness cells showed the lowest resistance of all the cells tested. Multiplying the capacitance, as measured by the slope of the linear portion of the constant current discharge curve (Eq. (2), with the resistance, measured by iR drop, gives the RC time constant. This data is summarized in Table 3. There is good agreement between the capacitances calculated from the two methods (see Eqs. (1) and (2)). This is explored in more detail in the section on electrochemical impedance spectroscopy (EIS).

The choice of electrolyte used in the supercapacitor has important consequences to the cell's behavior. In contrast to

Table 3
Comparison of measured capacitance, resistance, RC time constant, and solvent in electrolyte; values are the averages of at least three discharges

Manufacturer	Cell ID (number cells)	Capacitance from linear method (F)	Cell resistance from *iR* drop (mΩ)	RC time constant (s)	Major solvent in electrolyte
Saft	SAFT ($n = 1$)	3424	0.50	1.7	AN
Maxwell	PC2500 ($n = 2$)	3229	1.19	3.8	AN
CCR	CCR2000 ($n = 1$)	2439	2.40	5.8	PC
CCR	CCR3000 ($n = 1$)	2909	2.41	7.0	PC
Panasonic	UPC ($n = 2$)	1737	0.70	1.2	AN
Panasonic	UPA ($n = 2$)	1851	3.54	6.6	PC
Panasonic	UPB ($n = 2$)	982	2.30	2.3	PC
Ness	NESS ($n = 4$)	2444	0.47	1.1	AN
EPCOS	EPI2 ($n = 2$)	1202	1.23	1.5	PC

higher voltage lithium-ion batteries, supercapacitors have a cell voltage of less than 3 V. This allows a greater range of solvents to be used. Cells with acetonitrile-based electrolytes generally show better capacity and rate capability. For the cells tested in this study, Saft, Maxwell, Ness, and Panasonic UPC cells are acetonitrile-based. The other commonly-used solvent is propylene carbonate (PC). CCR, EPCOS and Panasonic UPA and UPB cells use PC. The difference in behavior between the two is significant, as can be seen by comparing Panasonic cells with acetonitrile (UPC) with those containing propylene carbonate (UPA) (see Fig. 1) which are otherwise similar.

6. Constant power (Ragone) results

The Ragone data on commercial supercapacitors and lithium-ion batteries are summarized in the following plot (Fig. 3). The data are normalized to the total cell weight. The striking result is the behavior of the Saft and Shin-Kobe lithium-ion batteries, both of which demonstrated remarkably high energy densities at high discharge power. Data from a Sony lithium-ion cell widely sold for consumer electronic devices and a Panasonic nickel-metal hydride cell (courtesy: Ramona Ying, GM-ATV) are included for comparison.

Comparison of the supercapacitor data shows that the Saft 3500 F supercapacitor showed the highest specific energy, consistent with Saft's self-reported results on 4000 F cells. The Power Systems and Panasonic UPC cells also showed a relatively high specific energy. The results on Maxwell's cells were in good agreement with those previously reported by Tim Murphy and Randy Wright at the Idaho National Engineering Lab on Maxwell cells [2]. The CCR cells showed slightly lower energy than Maxwell, which makes for an interesting comparison with the Peukert data, in which the specific capacities were comparable. The Panasonic UPA cells showed higher energy than the UPB cells. The Ness cells, similar to the constant current results, showed excellent power capability and a flat Ragone plot. The EPCOS and Panasonic UPB cells showed the lowest specific energy of the cells tested.

The PNGV goal of 25 kW pulse discharge power and 0.3 kW h total available energy are also plotted in Fig. 3 for comparison. These numbers were divided by the maximum allowable weight of 40 kg to give a goal of 625 W/kg specific power and 7.5 W h/kg specific energy. It should be noted, however, that the PNGV goal is for a pulse of 18 s.

The Ragone plot (Fig. 3) is for a constant power discharge from V_{max} to $0.5V_{max}$ in the case of the supercapacitors, and full discharge from V_{max} to V_{min} in the case of the lithium-ion cells. If the application does not require a full discharge from a fully charged state, the Ragone plot may not provide the most relevant information. Miller has advocated the use of an impedance-based approach to assess pulse power performance [8]. In this method, the reciprocal of the frequency f_0 at which the impedance has a -45° phase angle is defined as the characteristic response time T_0. The imaginary component Z'' (capacitance) at f_0 is used to calculate the available energy using the equation $E_0 = 0.5CV^2$, where $C = -1/(2\,\pi\, f_0\, Z'')$ and V is the rated voltage of the capacitor. The gravimetric "figure-of-merit" is simply the available gravimetric energy density (E_0/mass) divided by the characteristic response time T_0. This approach allows a direct and quantitative comparison between cells, without making assumptions regarding an equivalent circuit model.

To address the issue of a pulse rather than a continuous discharge, Miller has also suggested a "pulse power" Ragone method for assessing energy density with respect to power density for pulses of various durations [9]. The pulse power Ragone method uses electrochemical impedance spectroscopy data to develop an equivalent circuit model, which can be fed back into a SPICE-based modeling program to simulate pulses of different powers.

The results of the Ragone tests are summarized in tabular form below (see Table 4). This table, as with the Peukert table, takes two data points from each cell, the lowest and highest power discharge. The table lists the specific energy and specific power for those two points.

It is useful to compare the data obtained experimentally in this study with the theoretical calculations for expected results. Some researchers use a methodology where the maximum power at "matched impedance" [5] is calculated

Table 4
Summary of Ragone data at the lowest and highest power discharge

Manufacturer	Cell ID (number of cells)	Specific energy (W h/kg)	Specific power (W/kg)	Specific energy (W h/kg)	Specific power (W/kg)
Saft	SAFT ($n = 6$)	4.60	6.18	4.35	309.1
Maxwell	PC2500 ($n = 4$)	3.00	5.59	2.62	279.6
CCR	CCR2000 ($n = 3$)	2.89	9.51	1.90	474.3
CCR	CCR3000 ($n = 3$)	3.29	8.00	2.36	398.0
Panasonic	UPA ($n = 2$)	2.84	11.93	1.40	586.7
Panasonic	UPB ($n = 2$)	1.65	11.81	1.00	575.9
Panasonic	UPC ($n = 2$)	3.10	12.96	2.75	637.5
Ness	NESS ($n = 4$)	2.17	6.42	1.97	320.8
EPCOS	EP12 ($n = 2$)	1.56	4.17	1.45	222.3
Shin-Kobe	SK ($n = 8$)	41.42	13.27	34.08	663.6
Saft	HP6 (n=6)	74.41	10.77	62.04	520.3
Sony	NP ($n = 4$)	127.50	66.65	13.13	444.3
Panasonic	NiMH	49.71	14.71	32.25	588.2

for electrochemical capacitors. The matched impedance condition is when the load resistor is equal to the discharge ESR of the capacitor. With this load, the voltage immediately drops from V_0 to $0.5V_0$, and during the discharge, half of the energy is used to perform electrical work and the other half is released in the form of heat. The maximum power at matched impedance is given by the equation

$$P_{\mathrm{m}} = \frac{V_0^2}{4R} \tag{3}$$

where P is power, V_0 the initial voltage of the cell and R the cell's resistance. The discharge efficiency at this power is 50%. While this may be an interesting value for comparison, most applications will require considerably higher efficiency during actual operation. Power, as a function of efficiency, can be calculated using the cell voltage and resistance using the equation

$$P_{\mathrm{EF}} = \mathrm{EF}(1 - \mathrm{EF})\frac{V_0^2}{R} \tag{4}$$

where EF is the efficiency. The efficiency is less than 1.0 because the internal impedance of the cell generates some heat during discharge, thus reducing the amount of electric work performed. In the case of a cell discharged from V_0 to $V_0/2$, the peak power is given by

$$P_{\mathrm{EF}} = \frac{9}{16}(1 - \mathrm{EF})\frac{V_0^2}{R} \tag{5}$$

A table with theoretical energy density, power at 95% efficiency, and matched impedance power values is given below.

The theoretical energy density can also be calculated, if the cell's capacitance and maximum voltage are known using the equation $E = 0.5CV^2$. For a discharge range from $V_{\max}$ to $0.5V_{\max}$, the same as the experimental study, the theoretical value is 75% of the energy density calculated from a discharge to 0 V. The theoretical values show excellent agreement with the experimental results for the energy density (compare with Tables 4 and 5). The power densities are more difficult to compare because the experiment did not measure a 95% efficient discharge. The Saft cells showed the highest energy density, with Maxwell, CCR, and Panasonic UPC following, in that order. The Ness supercapacitors showed the lowest cell resistance and highest power density. The Saft and Panasonic UPC cells also exhibited high power density. This illustrates the need to select the device that is

Table 5
Theoretical energy density and power densities; theoretical energy density for a discharge from $V_{\max}$ to $0.5V_{\max}$ is given by $E = 0.75 \times 0.5CV^2$

Manufacturer	Cell ID (Number of cells)	Energy density (W h/kg)	Power density at 95% efficiency (W/kg)	Power density at matched impedance (W/kg)
Saft	SAFT ($n = 6$)	4.71	680	6045
Maxwell	PC2S00 ($n = 4$)	2.99	206	1835
CCR	CCR2000 ($n = 3$)	2.91	154	1371
CCR	CCR3000 ($n = 3$)	3.32	123	1097
Panasonic	UPAN ($n = 2$)	3.18	694	6166
Panasonic	UPA ($n = 2$)	2.93	125	1114
Panasonic	UPB ($n = 2$)	1.66	191	1698
Ness	NESS ($n = 4$)	2.21	512	4556
EPCOS	EP12 ($n = 4$)	1.76	324	2883

optimized for a specific application. For example, it is possible to design cells with thicker current collectors or more hardware designed to reduce internal impedance. This would result in a low ESR and high power density, but would also increase the weight and lower the energy density of the cell. As a reminder, the energy density for a discharge from V_{max} to $0.5V_{max}$, is only 75% of the energy density from V_{max} and 0 V. Therefore, the supercapacitors will exhibit higher energy density for applications that use the entire voltage range. Hybrid electric vehicle power-assist applications, however, restrict the voltage range from V_{max} to $0.5V_{max}$, which is how the data are presented in this paper. The power density is very dependent on the methodology used to calculate measured cell resistance R.

7. Electrochemical impedance spectroscopy measurements

Electrochemical impedance spectroscopy testing was conducted on the commercial supercapacitors. The results show that EIS is an effective tool for monitoring changes in the cell's impedance during the course of experiments or the cell's lifetime. In the EIS experiment, the cell is brought to the desired state of charge and held there for at least 1 h. Then, a sinusoidal voltage perturbation is applied to the cell at a well-defined frequency. The resulting current response is recorded and gives information regarding the electrochemical response of the system at that frequency. The process is repeated at various frequencies, typically ranging from 10 kHz to 1 mHz, for a given state of charge. Changes in EIS data can give important clues about the mechanisms in the cell behavior. For example, a Nyquist curve shifted to the right, with an otherwise similar shape, would suggest an increased series resistance.

When performing EIS measurements, it is important to minimize the impedance in the measurement system [10]. This is particularly true of supercapacitors, which have a very low internal resistance. Cabling and fixturing issues can lead to impedance that is not due to the cell, thus distorting the results. Care was taken in this investigation to minimize the impedance due to the measurement system by using the "pseudo" four-wire technique, as well as heavy copper bus bars to make electrical contact to the cells.

It is expected that the inability of an EC capacitor to satisfy the various tests at high current pulses may be due to increased internal impedance in the cell. Equivalent series resistance (ESR) is an important quantity in evaluating EC capacitors and is usually included in data sheets describing a cell's properties. However, the method used to measure the ESR is often not stated. If the behavior of the cell were purely capacitive, then the equivalent series resistance would not vary at different frequencies. Thus, a cell might be represented by a resistor in series with a capacitor. In practice, however, cells do not act as ideal pure capacitors and ESR should be defined when reporting numbers. Current

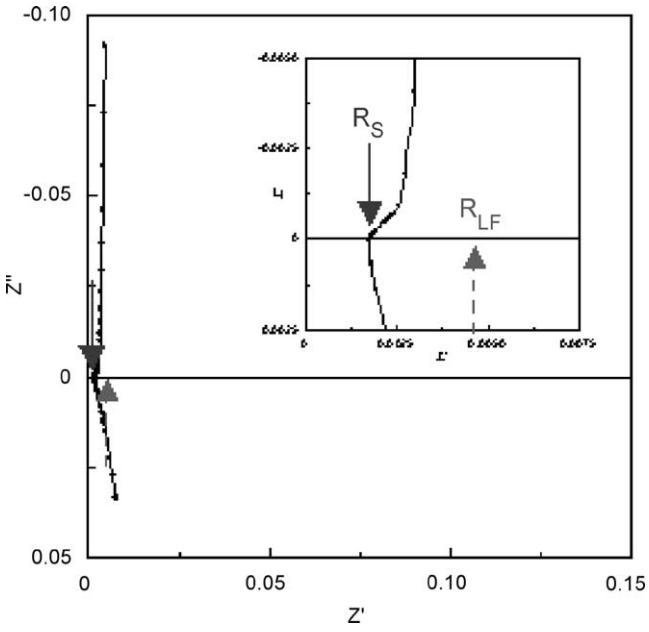

Fig. 4. Typical EIS Nyquist plot for a supercapacitor.

interrupt steps are commonly used to measure the internal resistance of the cell during an experiment. In this case, ESR is defined as the voltage change that occurs nearly instantaneously upon application of current: $\text{ESR} = \Delta V/\Delta I$. This method, however, is dependent on the methodology used, including the data sampling rate. Others define the ESR at a certain frequency.

Electrochemical impedance spectroscopy measurements are performed over a wide range of frequencies and therefore, can characterize the impedance of a cell, including processes with different time constants that may be occurring. A typical Nyquist plot of a supercapacitor cell is shown in Fig. 4. When analyzing the EIS data, the most common definition of ESR is the resistance at the crossover point on the Nyquist plot, or in other words the point where the curve crosses the Z'-axis, as $\omega \rightarrow \infty$. This is generally attributed to a very fast (instantaneous) series resistance since it occurs at a high frequency. In Figure, this corresponds to the blue arrow. At the other end of the frequency range, a low frequency resistance R_{LF} was defined as the real component of the impedance at the lowest frequency measured. Or, in other words, R_{LF} is the projection onto the Z'-axis. In Fig. 4, this corresponds to the red arrow. ΔR is the difference between these values.

To explore the behavior during constant current discharge, Fig. 2 is repeated here as Fig. 5. In, the constant current measurement data (shown by the solid, blue line) are compared to a simple equivalent circuit model (shown by the dashed, red line.) This simple equivalent circuit consists of a resistor in series with a capacitor. There are two measured resistances in this analysis: a "current interrupt" resistance and a "quasi static" resistance. The current interrupt resistance, as shown in Fig. 5, results in a nearly instantaneous drop in potential upon application of current.

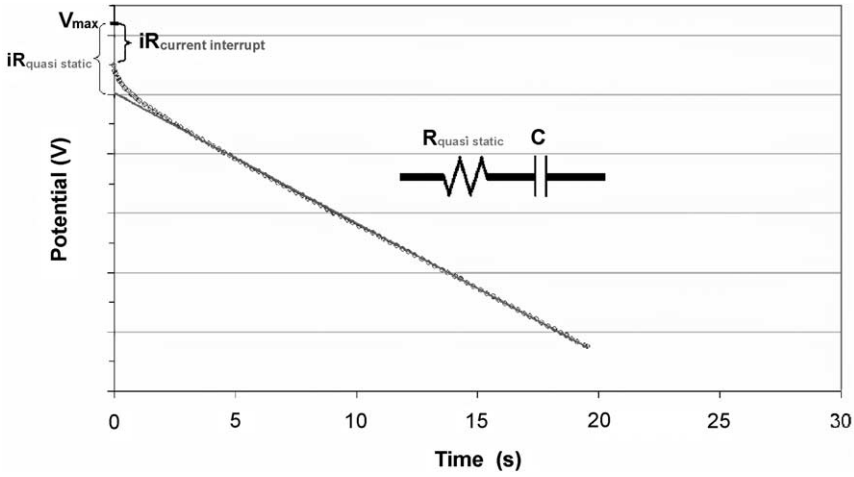

Fig. 5. Constant current discharge and equivalent circuit model.

This is a high frequency response. For the equivalent circuit model, the $R_{\text{quasi static}}$ is the resistance that would be predicted if the behavior of the cell could be fit using the simple two-element circuit. Since this can also be viewed as an extrapolation of the linear portion of the curve based on the longer time points, this might be viewed as a low frequency resistance.

Comparison of the constant current (Peukert) data with the EIS data shows a good correlation in measured resistances. Fig. 6 compares the high frequency resistance measured by the crossover in EIS Nyquist plots, with the resistance measured by instantaneous drop during the current interrupt method. There is very good correlation between the two, indicating that they are measuring the same phenomenon. Some of the discrepancy might be attributed to the difficulty in applying a large current or power pulse and in the resolution of the measurement. It is impossible for the tester to instantaneously apply the desired pulse, in a perfect square wave. Similarly, the accuracy of the resulting cell potential is dependent on the time resolution and the data sampling rate. Issues regarding the measurement of high power pulses at short time scales are not trivial and great care should be taken when conducting such measurements.

Fig. 7 compares the low frequency resistance measured by EIS, the low frequency projection of the real portion of the impedance, with the quasi-static resistance, as defined as the extrapolation of the linear portion of the constant current data. The correlation is not quite as good, given the scatter in the data. However, given the crude approximation the so-called quasi-static resistance represents, this can be considered good agreement.

Thus, either constant current or EIS method should be a good way to measure the internal resistance of the cell at high frequencies. However, care should be taken when comparing cells or values in the literature. This is especially an issue when an ‘‘equivalent series resistance’’ is reported. It is important to know how the measurement was taken. For example, if it was done by EIS, what frequency was used to determine the resistance? If it was a dc method, was it an instantaneous (high frequency) response? Furthermore, it may be important to note whether the quantity measured and reported is the most relevant for the application. For example, if the application requires a pulse of 30 s, but resistance

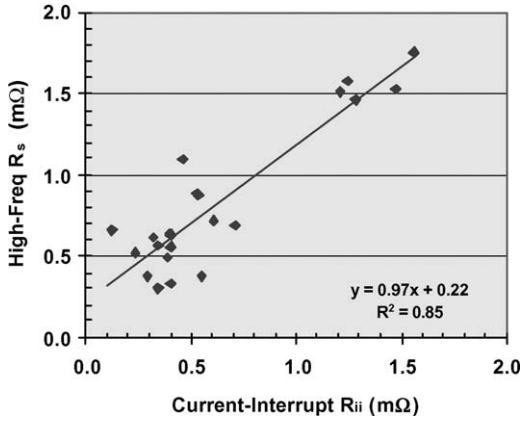

Fig. 6. High frequency R versus current interrupt R.

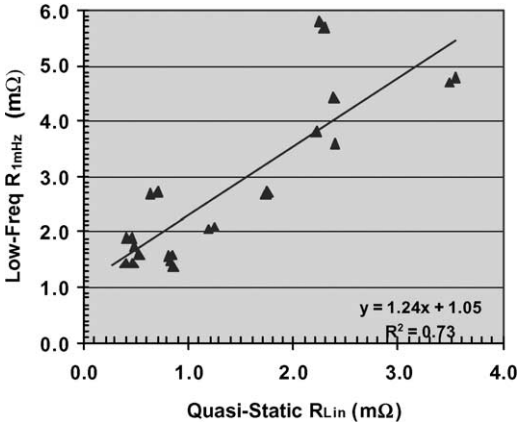

Fig. 7. Low frequency R versus quasi-static R.

is measured at high frequencies (corresponding to a time of a few milliseconds), the reported value may not be the most useful parameter.

The measured values of imaginary or real components of the impedance can be obtained by projecting them onto the *y*- and *x*-axes. In the calculation, the impedance is separated into real and imaginary components at a given frequency (1 mHz, in this case). The EIS "small-signal" capacitance is calculated from the imaginary component of the impedance using the equation:

$$C = \frac{1}{2\pi f Z} \tag{7}$$

where C is the capacitance, f the frequency and Z the imaginary component of impedance at frequency f.

The EIS capacitance was compared to the measured capacitance from the constant current experiment (using Eq. (2) for the commercial supercapacitors (see Fig. 8). Excellent agreement was found. When RC time constants were compared, as measured by both techniques, good agreement was found (see Fig. 9). The low frequency or quasi-static resistance was used, which may have contributed some scatter to the data. Nevertheless, it can be said that either EIS or the constant current linear approximation method do a good job of measuring a cell's resistance, capacitance, and RC time constant.

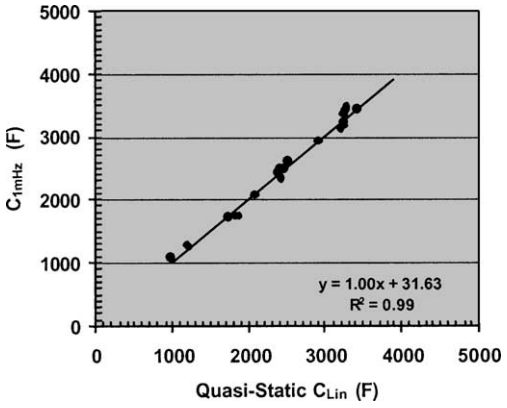

Fig. 8. Correlation of measured capacitance.

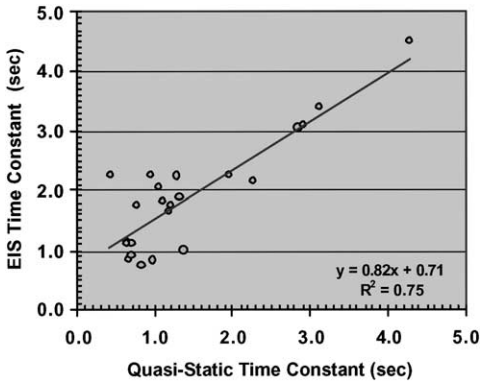

Fig. 9. Correlation of measured RC time constant.

8. Discussion

In this study, the authors chose generic testing methods, rather than those suggested by PNGV [11], because the PNGV test guidelines are not appropriate for testing supercapacitors. The program goals establish a set of performance criteria that define an "application space" for an appropriate energy storage system. HEV requirements tend to be so demanding that requirement-driven testing is necessary to determine whether any given energy storage system is even close to being appropriate for that application [12]. The PNGV process only works because it permits performance to be evaluated against all the goals more or less simultaneously. Certain types of batteries are well-suited to meet these specific criteria, whereas other types of energy storage systems (supercapacitors, for example) are not. This does not necessarily mean that supercapacitors are not well-suited for hybrid electric vehicle propulsion applications. However, the criteria by which cells are evaluated would need to be re-defined. Burke developed a supercapacitor test manual [13] to address this very concern.

Perhaps more problematic for developers of supercapacitors is the increased competition from today's high-power batteries. The current generation of lithium-ion batteries, for example, offers greatly superior rate and power capability, compared to earlier cells. Coupled with their inherently higher energy density compared to supercapacitors, these present the greatest challenge by setting a higher standard for any new technology to beat. Cost, however, remains an important issue and it is unclear at this time whether the cost of lithium-ion batteries will be low enough to permit their widespread use in production vehicles.

9. Conclusions

Supercapacitors have shown steady improvements in behavior in recent years. With a decreased internal resistance, a greater power density has been achieved. Despite these improvements, however, the energy density is still lower than desired for many applications, such as power-assist in hybrid electric vehicle propulsion. Although supercapacitors can not meet the PNGV requirements, this is partly due to the fact that the PNGV test methods are more appropriate for batteries. Supercapacitors and batteries occupy different application space. The use of supercapacitors must be made at the system level, not as a drop-in replacement to batteries.

Supercapacitors offer low resistance and fairly linear behavior. EIS and dc methods show good agreement in measured cell resistance. There does not appear to be significant hysteresis between charging and discharging behavior in fresh cells, besides the unavoidable, small potential (iR) drop. Cells with acetonitrile show better high-rate behavior than those with carbonate-based electrolytes.

Although supercapacitors have improved, newer high-power batteries, such as thin-film lead acid and lithium-ion

are offering power densities previously only achieved in electrochemical capacitors. Coupled with their greater capacity and energy, these cells are offering a significant challenge to developers of electrochemical capacitors. Corrosion and long-term stability are problems for thin-film lead acid. The high power lithium-ion batteries are currently quite expensive and supercapacitors might offer an edge in cost. To be competitive in hybrid electric vehicle applications, electrochemical capacitors must have increased energy density (>10 W h/kg) at a lower cost (<US$ 10 per kW).

It is possible that supercapacitors will show superior cycle life compared to batteries, including at elevated temperatures. However, further testing is required and in fact, will be the subject of a future paper. Cells with acetonitrile have shown lower resistance and higher energy and power densities, although the safety of such cells has not been demonstrated. Concerns regarding the use of acetonitrile must be addressed by manufacturers before its widespread acceptance can be expected. Failure modes and effects analysis (FMEA) must be conducted by suppliers. Only by addressing the open issues of energy density, cost, and failure modes, can supercapacitors find success in hybrid electric vehicle power-assist applications.

Acknowledgements

This work was funded by General Motors. Special thanks to Souren Soukiazian and John McHardy for their assistance.

References

[1] B.E. Conway, Electrochemical supercapacitors: scientific fundamentals and technological applications, Kluwer Academic Publishers/Plenum Publishers, New York, 1999, pp. 11–15.

[2] R.B. Wright, T.C. Murphy, Characterization of carbon-based electrochemical capacitor technology from Maxwell Energy Products Inc., Idaho National Engineering Laboratory, US Department of Energy, DOE/ID-10634, April 1998.

[3] R.B. Wright, T.C. Murphy, Characterization of carbon-based electrochemical capacitor technology from SAFT America Inc., Idaho National Engineering and Environmental Laboratory, US Department of Energy, INEEL/EXT-98-00818, August 1998.

[4] A. Burke, M. Miller, Characteristics of advanced carbon-based ultracapacitors, in: Proceedings of the 10th International Seminar on Double-layer Capacitors and Similar Energy Storage Devices, Deerfield Beach, FL, 2000.

[5] A. Burke, J. Power Sources 91 (2000) 37–50.

[6] L. Moreau, D. Cesbron, A. Chaillet, C. Jehoulet, Supercapacitors: power buffer for automotive applications, in: Proceedings of the 10th International Seminar on Double-layer Capacitors and Similar Energy Storage Devices, Deerfield Beach, FL, 2000.

[7] A.F. Burke, M. Miller, Comparisons of the power characteristics of ultracapacitors and batteries, in: Proceedings of the 8th International Seminar on Double-layer Capacitors and Similar Energy Storage Devices, Deerfield Beach, FL, 1998.

[8] J.R. Miller, Pulse power performance of electrochemical capacitors: technical status of present commercial devices, in: Proceedings of the 8th International Seminar on Double-layer Capacitors and Similar Energy Storage Devices, Deerfield Beach, FL, 1998.

[9] J.R. Miller, S.M. Butler, Electrochemical capacitor pulse power performance, in: Proceedings of the 10th International Seminar on Double-layer Capacitors and Similar Energy Storage Devices, Deerfield Beach, FL, 2000.

[10] M. Sandoval, G. Boyle, J. Munk, Four wire connection for performance measurement of low ESR devices, in: A. Burke (Ed.), Proceedings of the 10th International Seminar on Double-layer Capacitors and Similar Energy Storage Devices, Deerfield Beach, FL, 2000.

[11] PNGV Battery Test Manual, Revsion 3, Idaho National Engineering & Environmental Laboratory, US Department of Energy, DOE/ID-10597, February 2001.

[12] G. Hunt, Personal communication, February 2001.

[13] A. Burke, Electric Vehicle Capacitor Test Procedures Manual, Idaho National Engineering Laboratory, US Department of Energy, DOE/ID-10491, October 1994.